Hindawi
Discrete Dynamics in Nature and Society
Volume 2019, Article ID 2745381, 17 pages
https://doi.org/10.1155/2019/2745381

Research Article

Driving Anger States Detection Based on Incremental Association Markov Blanket and Least Square Support Vector Machine

Ping Wan,[1,2] Chaozhong Wu,[2] Yingzi Lin,[3] and Xiaofeng Ma [2]

[1] *The College of Transportation and Logistics, East China Jiaotong University, Nanchang, Jiangxi, 330013, China*
[2] *Intelligent Transport Systems Research Center, Wuhan University of Technology, Wuhan, Hubei, 430063, China*
[3] *Intelligent Human-Machine Systems Laboratory, Department of Mechanical and Industrial Engineering, Northeastern University, MA, 02115, USA*

Correspondence should be addressed to Xiaofeng Ma; maxiaofeng@whut.edu.cn

Received 30 August 2018; Accepted 28 February 2019; Published 26 March 2019

Academic Editor: Luca Pancioni

Driving anger, known as "road rage", has gradually become a serious traffic psychology issue. Although driving anger identification is solved in some studies, there is still a gap in driving anger grading which is helpful to take different intervening measures for different anger intensity, especially in real traffic environment. The main objectives of this study are: (1) explore a novel driving anger induction method based on various elicitation events, e.g., traffic congestion, vehicles weaving/cutting in line, jaywalking and red light waiting in real traffic environment; (2) apply incremental association Markov blanket (IAMB) algorithm to select typical features related to driving anger states; (3) employ least square support vector machine (LSSVM) to identify different driving anger states based on the selected features. Thirty private car drivers were enrolled to perform field experiments on a busy route selected in Wuhan, China, where drivers' anger could be induced by the elicitation events within limited time. Meanwhile, three types of data sets including driver physiology, driving behaviors and vehicle motions, were collected by multiple sensors. The results indicate that 13 selected features including skin conductance, relative energy spectrum of β band of electroencephalogram, standard deviation (SD) of pedaling speed of gas pedal, SD of steering wheel angle rate, vehicle speed, SD of speed, SD of forward acceleration and SD of lateral acceleration have significant impact on driving anger states. The IAMB-LSSVM model achieves an accuracy with 82.20% which is 2.03%, 3.15%, 4.34%, 7.84% and 8.36% higher than IAMB using C4.5, NBC, SVM, KNN and BPNN, respectively. The results are beneficial to design driving anger detecting or intervening devices in intelligent human-machine systems.

1. Introduction

Compared to vehicle and environment factors, such as sudden mechanical breakdown, slippery road and low visibility, human factors are found to be the most significant to traffic accidents [1]. Except for drunk driving, chatting with others, talking over a mobile phone, fatigue and distraction, driver's emotion is an important human factor to safe driving in a complex driver-vehicle-environment system [2]. Dahlen et al. [3] concluded that the most common emotion influencing traffic safety was driving anger. Driving anger, also called "road rage", is a special emotion induced by pressure or frustration caused by adverse driving environments or discourteous behaviors from traffic participants around [4]. Road rage has become increasingly common currently, threatening traffic safety around the world. A statistics report from American Automobile Association (AAA) in 2009 indicated that 5%-7% of 9282 surveyed drivers had outburst of road rage, among which, professional drivers like bus or truck drivers even reached 30% [5]. In China, a report showed that 60.72% of 9,620 surveyed drivers ever had road rage outburst experiences in daily life [6]. Generally, a driver's driving performance starts to deteriorate when he or she becomes angry while driving as anger has a negative impact on the driver's perception, identification, decision and volition process [3]. Furthermore, many aggressive behaviors, even traffic accidents have close relationship with driving anger [7]. According to statistics of National Highway Safety

Administration of U.S.A from 2007 to 2009, the number of the traffic accidents related with emotional driving including road rage accounted for about 9.2%~14.8% of the total [8]. An angry driver is apt to make more mistakes, lapses and violations, which causes more involvement in a traffic accident [9]. Hence, driving anger detection method should be developed to make target-specific intervening/warning for road rage.

In order to effectively and efficiently recognize different emotion states, it is critical to select adequate features which can accurately express the emotion states and, a suitable recognition method to identify them. In addition, for emotion recognition research, proper emotion induction approach is also needed. Correspondingly, a brief review of related studies regarding the aforementioned aspects is shown in the following paragraphs.

Effective emotion induction is an important precondition for emotion recognition researches, and it has often been addressed under laboratory conditions considering convenience and lower cost. Suarez et al. [10] firstly proposed a deception-based method to elicit anger in lab settings. Nonetheless, the method was executed with elaborate choreography to hide real aim of the experiments, which led to ethical concerns. Kessous et al. [11] induced several emotions including anger, fear, amusement and sadness according to speech-based interaction with an agent by pronouncing a sentence in a particular context. Juslin et al. [12] explored a music-based anger induction method through different combinations of positive/negative valences and high/low energy of music. Their results indicated that negative music with high energy could elicit the highest-level anger. Except for general emotion elicitation, there exist some researches about driving emotion elicitation. Lei et al. [13] chose film clips from famous films such as "Fist of Fury" and "The Rape of Nanking" to elicit anger for studying Chinese motorist's vehicle speed features in anger state. Abdu et al. [14] studied the differences of a driver's skilled driving behavior and risk taking behavior between neutral state and anger state which was induced in a quiet laboratory by recalling angry events happened in their daily life as vividly as possible. Cai et al. [15] elicited driving anger state by driver-to-driver interactions including blocking or changing lane abruptly in front of the subject car by using multiple networked driving simulators. However, the emotion induction in those studies is mainly completed under laboratory condition by using music, pictures, videos, elicitation scenarios or events designed in a driving simulator, which is likely to limit the generalizability of the induction methods because of personal preference or individual cultural background. Also, due to some demand characteristics and social desirability, the emotion induced under laboratory condition is less valid as that induced in real traffic environment [16]. Moreover, the induced emotions will drift away during driving process in a simulator, making arousal level of the induced emotions not high enough for emotion recognition.

Currently, emotion recognition is mainly based on features selected from facial expression, voice, posture (behavior) and physiology [17]. SÖnmez et al. [18] applied principal component analysis (PCA) and linear discriminant analysis (LDA) to select 60 eigenvectors from facial images to classify several basic emotions. Shahzadi et al. [19] implemented a hybrid filter and wrapper feature selection algorithm based on genetic algorithm (GA) to determine the most relevant prosodic features and spectral features of speech signals for emotion recognition. Kessous et al. [11] employed a wrapper subset evaluation method based on learning scheme to select several important characteristics of body posture movements such as motion quantity and contraction index and velocity of hand barycenter. For the sake of emotion recognition, Healey selected most significant physiological characteristics including heart rate (HR) and respiration amplitude by using t-tests and analysis of variance comparisons [20]. Wagner et al. [21] utilized sequential forward selection (SFS) algorithm to select the best feature set extracted from physiological signals to discriminate different emotions. Lee et al. [22] adopted mutual information (MI) technique to select features from electroencephalogram (EEG) and respiration signals for detecting sleepy driving state. In order to select best physiological features for emotion recognition, sequential backward selection (SBS) and Fisher projection method were employed by Wu et al. [23]. Chen et al [24] adopted the Markov blanket technique to propose a novel class-dependent feature selection model to improve the performance of speech emotion recognition with significantly reducing the feature dimensionality and obtaining better classification accuracy. Yan et al [25] used a Markov blanket-based method to select five effective vehicle motion features including speed, longitudinal acceleration and lane departure to recognize different driving risk status with Hidden Naïve Bayes. Han et al [26] proposed a new and fast Markov blanket-based method, FEPI-MB (fast Epistatic interactions detection using Markov blanket) to identify SNPs (single-nucleotide polymorphisms) disease with time-efficiency and better performance.

On the other hand, machine learning algorithms have been widely used for feature identification in many fields with data from multiple sensors, especially in emotion recognition research. Flidlund et al. [27] firstly recognized different emotions such as pleasure, anger, sadness and fear based on a linear discriminants method by using electromyography (EMG) features of facial expressions. Wang et al. [28] proposed a factorization model to recognize multiple driving emotions with several physiological features extracted from skin conductance (SC), blood volume pulse (BVP), respiration rate (RR), etc. Katsis et al. [29] utilized decision tree (DT) and Naïve Bayesian classifier (NBC) to identify car-racing drivers' emotional states including low stress, high stress, dysphoria, and euphoria with features of facial EMG, electrocardiogram(ECG), electrodermal activity (EDA) and respiration in simulated racing environment. Fan et al. [30] adopted Bayesian Network to identify driver emotion using EEG features including relative power spectrums from beta, alpha, theta and delta band, taking driver personality and traffic situation into consideration. Besides the physiological indicators for driving emotion recognition, driving behaviors and vehicle motions have been gradually used. Malta et al. [31] identified driver's frustration state according to EDA and brake/gas pedal actuation by using Bayesian network.

Lanatà et al. [32] employed nearest mean classifier (NMC) to discriminate two different driving stress levels using physiological indicators consisting of heart rate variability, respiration activity, and electrodermal response (EDR) along with mechanical information such as steering wheel angle corrections, velocity changes, and time responses. Rigas et al. [33] proposed Bayesian networks (BN) for driver's stress event detection by using physiological features including EDA, ECG and RR, as well as past observations of driving behaviors including speed, acceleration and heading. Other classification algorithms, such as the decision tree (C4.5), back propagation neural networks (BPNN) and k-nearest neighbor (KNN) are also widely used for driver mental state detection [34].

To date, most of the foregoing researches have focused on identifying several common emotions including happiness and stress and frustration in driving simulator environments. Few researches have been conducted with respect to detection of driving anger in real and complex traffic environment, particularly in the context of China, where road rage is an important issue seriously affecting road safety. Additionally, the foregoing researches have rarely focused on feature selection method for driving emotion detection, which requires much better feature selection effect than ordinary emotion recognition, considering effectiveness and efficiency for real-time detection in multi-sensors based application. Furthermore, for driver emotion recognition researches, most of previous studies roughly focused on two confused states (e.g. fatigue or not fatigue), without subdivision of a certain emotion state based on its intensity, which is necessary to take different intervening or relieving measures to address it. Moreover, the listed emotion recognition methods need to be improved for better accuracy in real-time applications.

Aimed at those, a high-arousal driving anger induction approach is firstly proposed based on the stimulation events naturally occurring in real traffic environment. Secondly, incremental association Markov blanket (IAMB) is introduced to determine the most effective features to express driving anger states with different intensity. Thirdly, least square support vector machine (LSSVM) approach is employed to propose a detection model of the driving anger states. Finally, classification performance of the proposed model is evaluated, compared with other identification models.

2. Materials

2.1. Participants. As males are more likely to get angry while driving than females [35], only male subjects were selected to perform experiments so as to maximize statistical power. Then, thirty male private car drivers were enrolled from Wuhan, China to conduct the field experiments. Those enrolled subjects have an average age of 38.6 years with a SD of 5.6 years, and an average driving experience of 10.2 years with a SD of 4.8 years. All subjects were medically evaluated prior to the study, and were found to be in good physical condition, which is very important when extracting their physiological features. Every subject was paid 300RMB (Chinese currency) after accomplishing the experiment. Besides, in order to record and evaluate each subject's self-reports of emotional state, and to guarantee safety during the whole experiments, an observer with rich driving experience (>20 yeas) was enrolled to be seated in co-driver position.

2.2. Apparatus. A car mounted with vehicle's controller area network (CAN)-bus was employed as the test vehicle for the field experiments (see Figure 1(a)), which collected data of driving behaviors such as steering wheel movement, gas and brake pedaling. Besides, the test car was equipped with many apparatus and sensors. For example, Mobileye C2-270 system (see Figure 1(b)) and Inertial Navigation System (see Figure 1(c)) were installed to acquire lane departure and speed/acceleration, respectively. NeuroScan4.5 acquisition system, consisting of a 32-channel-electrode cap, a NuAmp amplifier and acquisition software (see Figure 1(d)), was used to gather every subject's EEG signals. BioGraph Infiniti System consisting of ProComp Infiniti system and BioGraph software (see Figure 1(e)) was used to collect the subjects' physiological signals such as blood volume pulse (BVP), heart rate (HR), skin conductance (SC), finger temperature (FT), respiration amplitude (RA) and respiration rate (RR) by sensors taped on the subject's fingers and stomach, respectively. In summary, the apparatus system proposed in this study can acquire driver physiological signals, driving behaviors and vehicle motions signals. The corresponding acquisition apparatus and sampling frequency are all briefly introduced, as shown in Table 1.

Additionally, a seven-point scale from 0(not at all) to 6(very much) was used for recording levels of five possibly common emotions (anger, happiness, sadness, fear and calmness) while driving, which is important information to train and validate driving anger detection model proposed in this study. Last but not least, three high definition cameras mounted on the front windshield of the test vehicle (see Figure 1(f)) were used to shoot driving environments (stimulation events) ahead, the subjects' facial/phonetic expression and their general situations of operational behaviors (i.e. amplitude and frequency) on steering wheel, gas/brake pedal and gear lever, respectively. The video replay could be used as auxiliary evidence for emotion labeling when a subject's self-reports gravely deviated from the observer's evaluation. The overall sketch of apparatus system was shown in Figure 1(g).

2.3. Experiment Design. A specific test route including heavy traffic sections across Wuchang and Hankou Districts of Wuhan city was chosen to induce the subjects' anger as much as possible, (see Figure 2(a)). The test route, 51 kilometers long, consisted of 42 signalized intersections, 59 pedestrian crosswalks, two expressways, two tunnels and three large-scale business districts. When driving on the test route, the subjects would frequently encounter many random elicitation events including vehicles weaving/cutting in line, jaywalking, traffic congestion and red light waiting, especially during morning or evening rush hours (see Figure 2(b)). Therefore, after one-hour preparation with physiological equipment wearing/configuring and driving practice, every subject was demanded to start their experiments at about 8:00 a.m. or 5:00 p.m. In order to enhance anger induction effect, every subject would get additional paid with 15RMB/min if

(a) Test car for on-road experiments

(b) Mobileye C2-270 system

(c) Inertial Navigation RT 2500 System

(d) NeuroScan4.5 acquisition system

(e) BioGraph Infiniti System

(f) Monitor video camera system

(g) Overall sketch of the apparatus system

Figure 1: The Apparatus of field experimental system [36].

they accomplish the test ahead of schedule (120 minutes), which is verified to provide a little pressure for the subjects for the accomplishment.

2.4. Experiment Procedure. First, every subject was asked to sign an informed agreement interpreting experiment requirements. It is noted that all subjects are forbidden to break any traffic regulation, especially speeding. Second, after wearing and configuring all the apparatus, especially the physiological signals acquisition system, every subject did ten-minute driving practice to adapt to the apparatus as well as the test vehicle. Third, when the formal test began, every two minutes during the experimental process or any moment an anger elicitation event occurred, the subject was surveyed by the observer through a very simple question(the question is too simple to interference the subject [37]), "How do you feel in the last 2 minutes" or " How do you feel just now?" And they had to respond to evaluate which emotion he felt the most and how intensely through the seven-point scale. Meanwhile, the observer also evaluated the subject's emotional state according to his facial/phonetic expression and general situation of driving behaviors including steering wheel and gear lever movement by the same scale. Besides the subject's self-response, physiology, driving behaviors and vehicle motions were recorded during the whole experiment. In this study, ambient temperature and noise of the test vehicle were controlled to be 18±2°C and 60±5dB, respectively, in order to eliminate the influences of these factors on physiological signals. Note that the experimental tests on those subjects conformed to Chinese laws relating to scientific research.

3. Methods

3.1. Data Preprocessing. As introduced in the aforementioned section of apparatus, a total of four types of data including driving anger levels, driver physiology, driving behaviors and vehicle motions need to be preprocessed.

When dealing with driving anger levels, any subject's self-report levels would be directly used as his final anger

Table 1: Brief introduction of multisensors based data collection.

Indicators	Apparatus (Sensors)	Sampling frequency	Tag
Physiological measures			
BVP	BioGraph Infiniti System	256Hz	BVP
SD of BVP	BioGraph Infiniti System	256Hz	SBVP
HR	BioGraph Infiniti System	256Hz	HR
SD of HR	BioGraph Infiniti System	256Hz	SHR
SC	BioGraph Infiniti System	256Hz	SC
SD of SC	BioGraph Infiniti System	256Hz	SSC
RA	BioGraph Infiniti System	256Hz	RA
SD of RA	BioGraph Infiniti System	256Hz	SRA
RR	BioGraph Infiniti System	256Hz	RR
SD of RR	BioGraph Infiniti System	256Hz	SRR
ST	BioGraph Infiniti System	256Hz	ST
SD of ST	BioGraph Infiniti System	256Hz	SST
δ%	NeuroScan4.5 system	1000Hz	δ%
SD of δ%	NeuroScan4.5 system	1000Hz	Sδ%
θ%	NeuroScan4.5 system	1000Hz	θ%
SD of θ%	NeuroScan4.5 system	1000Hz	Sθ%
α%	NeuroScan4.5 system	1000Hz	α%
SD of α%	NeuroScan4.5 system	1000Hz	Sα%
β%	NeuroScan4.5 system	1000Hz	β%
SD of β%	NeuroScan4.5 system	1000Hz	Sβ%
Driving behaviors			
Steering wheel angle	Vehicle CAN system	60Hz	SWA
SD of steering wheel angle	Vehicle CAN system	60Hz	SSWA
steering wheel angle rate	Vehicle CAN system	60Hz	SWAR
SD of steering wheel angle rate	Vehicle CAN system	60Hz	SSWAR
pedaling depth of gas pedal	Vehicle CAN system	60Hz	PDGP
SD of pedaling depth of gas pedal	Vehicle CAN system	60Hz	SPDGP
pedaling speed of gas pedal	Vehicle CAN system	60Hz	PSGP
SD of pedaling speed of gas pedal	Vehicle CAN system	60Hz	SPSGP
pedaling depth of brake pedal	Vehicle CAN system	60Hz	PDBP
SD of pedaling depth of brake pedal	Vehicle CAN system	60Hz	SPDBP
pedaling speed of brake pedal	Vehicle CAN system	60Hz	PSBP
SD of pedaling speed of brake pedal	Vehicle CAN system	60Hz	SPSBP
Vehicle motions			
Speed	Vehicle CAN system	60Hz	SP
SD of speed	Vehicle CAN system	60Hz	SSP
lateral velocity	Inertial Navigation System	100Hz	LV
SD of lateral velocity	Inertial Navigation System	100Hz	SLV
forward acceleration	Inertial Navigation System	100Hz	FA
SD of forward acceleration	Inertial Navigation System	100Hz	SFA
lateral acceleration	Inertial Navigation System	100Hz	LA
SD of lateral acceleration	Inertial Navigation System	100Hz	SLA
heading angle	Inertial Navigation System	100Hz	HA
SD of heading angle	Inertial Navigation System	100Hz	SHA
heading angle rate	Inertial Navigation System	100Hz	HAR
SD of heading angle rate	Inertial Navigation System	100Hz	SHAR
Rolling angle rate	Inertial Navigation System	100Hz	RAR
SD of Rolling angle rate	Inertial Navigation System	100Hz	SRAR
time headway	Mobileye C2-270 system	8Hz	THW
SD of time headway	Mobileye C2-270 system	8Hz	STHW
lane departure	Mobileye C2-270 system	8Hz	LD
SD of lane departure	Mobileye C2-270 system	8Hz	SLD

(a) The test route (shown as blue line) (b) Elicitation events in real traffic environment

Figure 2: The test route and traffic environment of field experimental system [36].

level if the evaluation difference between him and the observer is less than 2. Or else, three more independent experts (research assistants) in driving behavior, with much driving experience will be requested to evaluate the subject's anger level according to the replays of videos shot during the experimental process. And those directly accepted self-reports on the subjects' anger levels were used as the baseline for the three experts' evaluations.

In the aspect of physiological signals such BVP and SC, some artifacts will be generated due to movements of hands. Thereby, the artifacts were removed according to data distribution in boxplot. Particularly, as the designed experiments were conducted in real traffic environment, raw EEG data was mixed with numerous noises, among which high frequency noise is due to atmospheric thermal noise while low frequency noise is mainly due to eye movements, respiration and heart beats. Then, the high and low frequency noise were filtered through band pass filter with cutoff frequencies of 0.5 Hz and 35 Hz, as well as a method based on independent component analysis [38].

With respect to data preprocess for driving behaviors and vehicle motions, a cubic spline interpolation, has been proved to be a viable method to restore the invalid, outlying and time-related errors due to instability of the data acquisition system in complex traffic environment. Last but not least, synchronization work is of great importance to be done for all types of data listed above.

Based on the survey from the subjects and video records, their anger level can be generally maintained in the first 6~10 seconds after stimulation of the anger elicitation events, then it reduces if no more elicitation events happen. Hence, the three kinds of measurements including physiology, driving behavior and vehicle motion signals lasting for 8 (i.e. (6+10)/2) seconds from the moment the elicitation events happened were selected for the study on driving anger states, while the three kinds of measurements with the same time span in neutral state were selected for the study on none anger state.

3.2. Anger Intensity Labeling

3.2.1. Emotion Induction Performance. As the subjects may experience different emotions throughout the test route, an evaluation is needed to check whether the subjects' self-reported emotions match well with target emotion (i.e. anger). In this study, occurrence rate of anger was introduced as an indicator to evaluate emotional differentiation degree. Every subject had to report his emotion level every two minutes and the moment an elicitation event happened during experimental process, so a total of 1861 emotion self-reports were collected from all subjects including 906 anger emotion instances, and 713 calm (neutral) instances. As shown in Table 2, anger occurrence rate is only 8.83% if no anger elicitation events happed while driving, which might result from award of completing experiment ahead of time. Comparatively, occurrence rate of anger under stimulation of jaywalking/cyclist crossing can reach its maximum 80.27%, while the minimum 55.03% under stimulation of waiting red light, which is significantly bigger than that without stimulation of the elicitation events. Summarily, occurrence rate of anger under the elicitation events reaches 72.22% (i.e. (906-61)/(1861-691)), significantly higher than that (8.08%) under no elicitation events. Consequently, the novel anger induction method proposed in this study can be considered to be feasible based on the elicitation events.

3.2.2. Anger Intensity Labeling and Relevant Trigger Events. In order to tackle road rage issue before it threatens traffic safety, driving anger warning or intervening measures corresponding to specific anger intensity is of great importance. Thus, different anger intensity should be labeled according to the anger levels self-reported by all subjects. In this study, in terms of anger intensity, all driving states were classified into four categories which included none anger state (anger level < 1), low anger state ($1 \leq$ anger level < 3), medium anger state ($3 \leq$ anger level < 5) and high anger state (anger level ≥ 5). Therefore, 906 anger-related samples and 713 neutral (i.e. none anger) samples, were acquired for this study. The number distribution of those samples is illustrated in Figure 3. Moreover, that plenty of medium and high anger samples were stimulated proves that the anger induction method put forward in this study is feasible.

After labeling the driving anger intensity, the stimulation events which triggered the relevant driving anger state and the times of the driving anger state triggered by the relevant stimulation events are obtained, listed in Table 3. As indicated

Table 2: Occurrence rate of five emotions from the scenarios with and without anger elicitation events.

Elicitation events	*fear*	*happy*	*anger*	*Sad*	*Neutral*	*Total*	*Occurrence rate*
Without anger elicitation	7	33	61	5	585	691	8.83%
jaywalking/cyclist crossing	37	3	293	9	23	365	80.27%
Weaving/cutting in line	45	4	278	18	30	375	74.13%
Traffic congestion	16	6	181	24	34	261	69.35%
Waiting red lights	11	5	93	19	41	169	55.03%
Total	116	51	906	75	713	1861	/

Table 3: The times of anger states triggered by the specific stimulation events.

Elicitation events	*High anger*	*Medium anger*	*Low anger*	*None anger*
Without anger elicitation	0	0	61	585
jaywalking/cyclist crossing	43	142	108	23
Weaving/cutting in line	82	125	71	30
Traffic congestion	23	27	131	34
Waiting red lights	13	21	59	41
Total	161	315	430	713

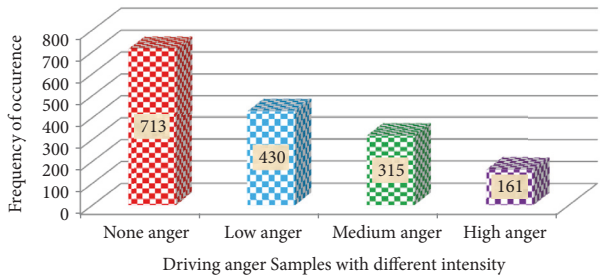

Figure 3: The number of different anger states.

in Table 3, high driving anger state is mostly caused by the surrounding cars' weaving/cutting in line behaviors, followed by jaywalking/cyclist crossing behaviors. Medium anger state is mostly caused by jaywalking/cyclist crossing behaviors while low anger state is mostly caused by traffic congestion. Moreover, in the light of waiting red light event, the event brought about more low anger states, when compared with the other anger states. Additionally, even the same stimulation events can induce different driving anger states because of the participants' individual personality/demographic characteristics differences such as age, gender, temperament, driving experience.

3.3. Markov Blanket Algorithm for Features Selection of Driving Anger States. As a large number of measures for driver physiology, driving behaviors and vehicle motions were acquired by various sensors, dimensionality reduction and feature selection from all various measures is strongly required for improving detection performance of driving anger states and reducing computation burden for real-time detection. Then Markov blanket algorithm was introduced to select most effective and efficient features to classify different driving anger states.

Koller et al. [39] firstly proposed Markov blanket (MB) algorithm for identifying redundant and irrelevant features based on cross-entropy theory. Relevant research indicated that determining Markov blanket of a target variable T was of key importance when selecting features [40, 41]. For example, the Markov blanket of target variable T, namely, a certain driving anger state, is the most effective and efficient set consisting of key features which have significant impact on T. Hence, The Markov blanket of target variable T, denoted as *MB (T)*, should be a minimal set of features conditioned on which all other variables are probabilistically independent of T, as shown in Definition 1[42].

Definition 1. Suppose a set of all attributes in the domain is denoted by F, and a feature subset MB_i, and $MB_i \in F$, then, MB_i is determined to be Markov blanket of target variable T_i, when the following equations are satisfied:

$$T_i \cap MB_i \neq T_i \tag{1}$$

$$P\left(F - MB_i - \{T_i\}, MB_i\right) = P\left(F - MB_i - \{T_i\} \mid MB_i\right) \tag{2}$$

where, $P()$ means the corresponding probability.

From the perspective of Bayesian network, the Markov blanket of T is comprised of the parents, the children and the parents of the children and the spouse nodes of the target T. Thus, *MB(T)* is sufficient to be used to calculate probability distribution of T for classification. In order to effectively and efficiently find *MB(T)*, incremental association Markov blanket (IAMB)algorithm [43, 44] is adopted in this study. The algorithm is implemented, as shown in Algorithm 1.

The IAMB algorithm, as shown in Algorithm 1, consists of two phases which include growing phase and shrinking phase. In the growing phase, the features which are calculated to be dependent of target variable T, are added to *MB (T)* by using independence test (line (1)-(6)). Then, according to this process, Markov boundary is determined. In the shrinking phase, any features among *MB(T)*, which are calculated to be independent of T, is removed from *MB(T)*(line (7)-(10)).

Input: Training dataset D(F, T) /∗ F is feature set and T is target variable∗/
Output: MB(T) /∗Markov blanket of T∗/
/∗add true positives to MB(T) ∗/
(1) MB(T) = ∅
(2) **repeat**
(3) Y = arg : $\max_{X\in(F\setminus MB\{T\})} dep(T, X \mid MB(T))$
(4) **if** (!(T ⊥ Y | MB(T)), **then**
(5) MB(T) = MB(T) ∪ {Y}
(6) until MB(T) does not change;
/∗ remove false positives from MB(T) ∗/
(7) **for each** X ∈ MB(T) **do**
(8) **if** T ⊥ X | (MB(T) \ {X}) **then**
(9) MB(T) = MB(T) \ {X}
(10) return MB(T).

Algorithm 1: The pseudocode of IAMB algorithm.

When completing the process, the redundant features of *MB(T)* are further eliminated.

3.4. Least Square Support Vector Machine Model for Detecting Driving Anger States

3.4.1. LSSVM Model. Cortes et al. firstly proposed support vector machine (SVM) method to address classification and regression problems [45]. SVM is a machine learning method which is based on statistical learning and minimization principle of structural risk. Particularly, the SVM method can tackle non-linear classification problem in higher-dimensional space by using best separating hyperplane. However, in order to relieve the defect of much time-consuming for quadratic programming during training process of SVM model, least square support vector machine (LSSVM) was put forward by Suykens [46]. The core idea of this algorithm is to adopt equality constraints instead of inequality constraints used in standard SVM learning process, which could improve solving speed and convergence precision of the standard SVM model [47].

For a given sample set (x_i, y_i) (i = 1, 2, . . . , k), x_i is input data and $x_i \in R^n$, y_i is output data and $y_i \in R$. The fitting function for the sample set is constructed as follows:

$$y(x) = \boldsymbol{\omega}^T \varphi(x) + \boldsymbol{b} \tag{3}$$

where, non-leaner mapping function $\varphi : R^n \longrightarrow R^{nh}$ can map the input data into a higher-dimension feature space. $\boldsymbol{\omega}$ is a weight vector, and $\boldsymbol{\omega} \in R^{nh}$; $\boldsymbol{b}$ is a bias vector, and $\boldsymbol{b} \in R$. To calculate $y(x)$, an objective function is defined as follows:

$$\min \quad J(\boldsymbol{\omega}, \boldsymbol{\xi}_i) = \frac{1}{2}\boldsymbol{\omega}^T\boldsymbol{\omega} + \frac{\lambda}{2}\sum_{i=1}^{k}\boldsymbol{\xi}_i^{\,2} \tag{4}$$

$$\text{s.t.} \quad y_i = \boldsymbol{\omega}^T\varphi(x_i) + \boldsymbol{b} + \boldsymbol{\xi}_i \tag{5}$$

where, λ is a constant, $\lambda \in R^+$; $\boldsymbol{\xi}_i$ is a slack variable. Subsequently, Lagrange function is described as the following:

$$L(\boldsymbol{\omega}, \boldsymbol{b}, \boldsymbol{\xi}_i, \boldsymbol{\beta}) = \frac{1}{2}\boldsymbol{\omega}^T\boldsymbol{\omega} + \frac{\lambda}{2}\sum_{i=1}^{k}\boldsymbol{\xi}_i^{\,2} - \sum_{i=1}^{k}\boldsymbol{\beta}_i\left[\boldsymbol{\omega}^T\varphi(x_i) + \boldsymbol{b} + \boldsymbol{\xi}_i - \boldsymbol{y}_i\right] \tag{6}$$

where, $\boldsymbol{\beta}_i$ is a Lagrange multiplier, according to Karush-Kuhn-Tucker (KKT) conditions:

$$\frac{\partial L}{\partial \boldsymbol{\omega}} = 0 \longrightarrow \boldsymbol{\omega} = \sum_{i=1}^{k}\boldsymbol{\beta}_i\varphi(x_i) \tag{7}$$

$$\frac{\partial L}{\partial \boldsymbol{b}} = 0 \longrightarrow \boldsymbol{b} = \sum_{i=1}^{k}\boldsymbol{\beta}_i = 0 \tag{8}$$

$$\frac{\partial L}{\partial \boldsymbol{\xi}_i} = 0 \longrightarrow \boldsymbol{\beta}_i = \lambda \cdot \boldsymbol{\xi}_i \tag{9}$$

$$\frac{\partial L}{\partial \boldsymbol{\beta}_i} = 0 \longrightarrow \boldsymbol{\omega}^T\varphi(x_i) + \boldsymbol{b} + \boldsymbol{\xi}_i - y_i = 0 \tag{10}$$

After eliminating $\boldsymbol{\omega}$ and $\boldsymbol{\xi}_i$, the analytical solution of the optimization problem is listed as follows:

$$\begin{bmatrix} \boldsymbol{b} \\ \boldsymbol{\beta} \end{bmatrix} = \begin{bmatrix} \boldsymbol{0} & \boldsymbol{1}^T \\ \boldsymbol{1} & \boldsymbol{K} + \lambda^{-1}\boldsymbol{I} \end{bmatrix}^{-1} \begin{bmatrix} 0 \\ y \end{bmatrix} \tag{11}$$

where, $\boldsymbol{\beta} = [\boldsymbol{\beta}_1, \boldsymbol{\beta}_2, \ldots, \boldsymbol{\beta}_k]^T$, $\boldsymbol{1} = [1, 1, \ldots, 1]^T$; the square matrix $\boldsymbol{K}$ satisfies the following:

$$K_{ij} = \varphi(x_i)^T\varphi(x_j), \quad i, j = 1, 2, \ldots, k \tag{12}$$

Further, the least square model is calculated as follows:

$$y(x) = \sum_{i=1}^{k}\boldsymbol{\beta}_i\boldsymbol{K}(x, x_i) + \boldsymbol{b} \tag{13}$$

where, $\boldsymbol{K}(x, x_i)$ is a kernel function, namely a symmetrical function which satisfies Mercer condition. As we know, the

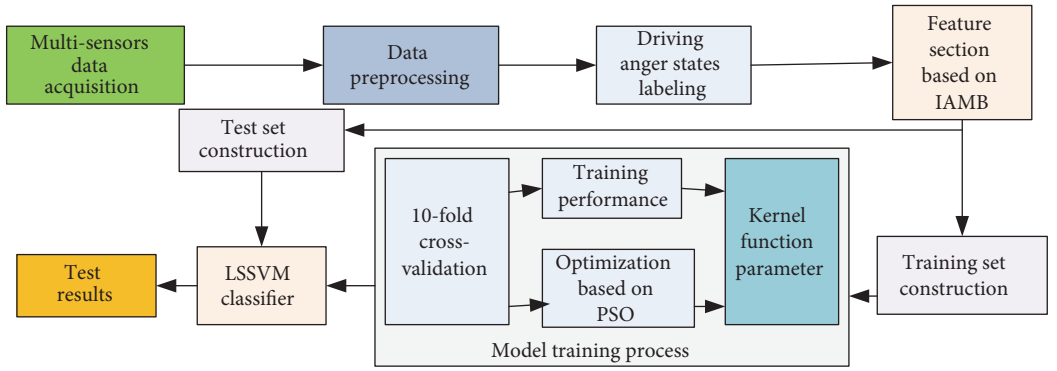

Figure 4: The modeling process of LSSVM with IAMB.

common kernel functions include linear, polynomial, radial basis function (RBF) and sigmoid. In this study, due to its good statistical ability, RBF kernel function is implemented as follows:

$$\boldsymbol{K}(x, x_i) = \exp\left[-\frac{\|x - x_i\|^2}{2\sigma^2}\right] \tag{14}$$

where, x and x_i denote the inputs in original space R^n and higher dimension space R^{nh}, respectively; σ is radius (i.e. width) of RBF kernel.

3.4.2. Parameter Optimization. As listed above, both kernel parameter σ and penalty parameter λ are important parameters of LSSVM model, which have significant impact on classification performance of the model. Here, for the sake of better classification performance, particle swarm optimization (PSO) is adopted to optimize the two parameters

The method of PSO, based on stochastic optimization of a population, is often used to simulate the social behavior of flocking organisms [48]. The process of PSO is conducted by cooperation and competition among all individuals of the population, and the potential solution of the optimization problem is represented by a special swarm of particles. The core idea of PSO is executed as the following two steps: (1) firstly, all particles are initialized by a random velocity and position; (2) each particle updates its position and velocity based on classification performance of the classifier.

It is noted that each particle moves in D-dimensional space at every iterative process, with the objective of finding the global optimum. During the process of searching global optimum, the best previous position (PB) of a specific particle will be generated based on its memory. Then the global optimum of the swarm, denoted by PG can be selected from those possible PBs. The updating process is conducted as follows [49]:

$$\begin{aligned} v_i(t+1) = {} & v_i(t) + \mu_{1i}\left(PB_i - S_i(t)\right) \\ & + \mu_{2i}\left(PG - S_i(t)\right) \end{aligned} \tag{15}$$

$$S_i(t+1) = S_i(t) + v_i(t+1) \tag{16}$$

where, i is particle index, t is time index; v_i is velocity of ith particle; $S_i(t)$ is position of ith particle; μ_{1i} and μ_{2i} are random constants with the range of 0 to 1. In this study, equation (15) can also be transformed as follows:

$$\begin{aligned} v_i(t+1) = {} & \tau(t)\, v_i(t) + \gamma_1\left[\mu_{1i}\left(PB_i - S_i(t)\right)\right] \\ & + \gamma_2\left[\mu_{2i}\left(PG - S_i(t)\right)\right] \end{aligned} \tag{17}$$

where $\tau(t)$ is inertia function; γ_1 and γ_2 are both acceleration constants.

Subsequently, a ten-fold cross validation method, together with PSO are applied to optimize the kernel parameter and the penalty parameter. Therefore, the overall driving anger detection process consists of the feature selection based on IAMB and the training and test process of LSSVM model, as shown in Figure 4.

3.5. Performance Evaluation for Detection Model

3.5.1. Construction Principle of ROC Curve. In order to evaluate the classification performance of LSSVM model proposed, an evaluation method of receiver operating characteristic (ROC) curve is introduced in this study. The evaluation method, deriving from detection theory for electrical signals, has been extensively applied in many fields such as medical diagnosis, human decision-making, military monitoring and industrial quality control [50–52]. As we know, identification evidence of most classifier is based on its output, which reflects the probability of a sample recognized as positive or negative ones. Hence, if we put all those probabilities in a monstrous increasing or decreasing order, and set each probability as a possible discrimination threshold (cut-off point), then true positive rate (TPR, i.e. sensitivity) and false positive rate (FPR, i.e. 1-specificity) can be obtained according to the following:

$$TPR = \frac{TP}{TP + FN} \tag{18}$$

$$FPR == \frac{FP}{TN + FP} \tag{19}$$

where, TP is the number of positive samples correctly classified; FP is the number of negative samples which are falsely classified into positive ones; TN is the number of negative samples correctly classified; FN is the number of

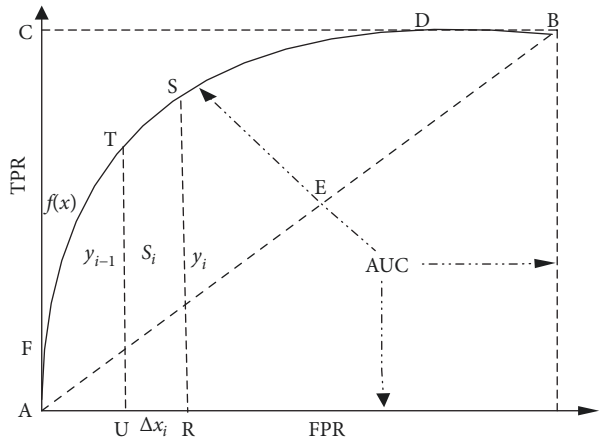

Figure 5: Schematic of ROC curve system [36].

positive samples which are falsely classified into negative ones. Here, driving anger samples with certain intensity is supposed to be positive while the other driving anger samples are supposed to be negative.

As shown in Figure 5, in the coordinate system for ROC curve, the horizontal ordinate and vertical ordinate of the cut-off point are denoted by *FPR* and *TPR*, respectively. If different cut-off points are implemented for classifying different driving anger states, a ROC curve will be produced via connecting those cut-off points with a line in the coordinate system (e.g. arc FD in Figure 5).

3.5.2. Calculation Principle of AUC. The classification performance of a specific classifier depends on the shape and position of the ROC curve in the coordinate system, illustrated in Figure 5. The most ideal ROC curve, namely, line AC or CB, means classification accuracy is 100%, and the sensitivity and specificity of all cut-off points are both 100%. However, in real application, the situation seldom happens, and then the ROC curve represented by arc *FD* is more typical. For any classification algorithm, its sensitivity and specificity cannot be improved at the same time, nonetheless, the area under the curve (*AUC*) of ROC can be served as an intuitional indicator to comprehensively evaluate classification performance, especially the number of positive samples and the number of negative samples are seriously unbalanced. The greater AUC is, the higher accuracy the classifier has. Here, the AUC can be calculated by means of integration of trapezoid URST (see Figure 5) [36], namely:

$$AUC = \int_e^f f(x)\,dx = \sum_{i=1}^{n} S_i = \sum_{i=1}^{n} \frac{y_{i-1} + y_i}{2} \Delta x_i \tag{20}$$

where, e and f are the lower and upper bound of x (i.e. FPR), respectively; S_i is area of the ith curved trapezoid (i.e. trapezoid URST) in the coordinate system; y_{i-1} and y_i are the length of upper base and lower base of trapezoid URST, respectively; Δx_i is the height of trapezoid URST.

Except for the criteria of TPR and FPR and AUC, positive predictive accuracy (PPA, called precision) and F1 and Accuracy (Acc) are three other criteria widely used to evaluate a classifier's performance, which are calculated as follows:

$$PPA = \frac{TP}{TP + FP} \tag{21}$$

$$F1 = \frac{2 \times TPR \times PPA}{TPR + PPA} \tag{22}$$

$$Acc = \frac{TP + TN}{TP + FN + TN + FP} \tag{23}$$

where, *TP*,*TN, FP* and *FN* can be referred to the definitions for Formula (18) and (19). Note that *PPA* demonstrates the probability of correct identification provided a positive classification of the specific emotion.

4. Results

4.1. The Result of Feature Selection. For the sake of selecting the most effective and efficient features which have significant impact on driving anger states, incremental association Markov blanket (IAMB) algorithm was applied with the selection results shown in Figure 6. As illustrated in Figure 6, the objective features (denoted by grey color), which have the strongest relationship with driving anger states, are comprised of 13 features including skin conductance (SC), SD of heart rate (SHR), SD of respiration rate (SRR), relative energy spectrum of θ band of EEG (θ%), relative energy spectrum of β band of EEG (β%), SD of pedaling speed of gas pedal (SPSGP), SD of steering wheel angle (SSWA), SD of steering wheel angle rate (SSWAR), SD of heading angle rate (SHAR), vehicle speed (SP), SD of speed (SSP), SD of forward acceleration (SFA) and SD of lateral acceleration (SLA). These grey features thus can be utilized for driving anger states detection. Moreover, the relationship between the objective features and other features is also illustrated in Figure 6.

Further, in order to verify whether the selected features (i.e. objective features) have significant correlations with the corresponding driving anger state, Kendall's tau-b and Spearman's rho coefficient tests are implemented, as shown in Table 4. From Table 4, it can be concluded that SC, SHR, SRR, θ%, β%, SPSGP, SSWA, SSWAR, SHAR, SP, SSP, SFA and SLA are all significantly correlated with different driving anger states, when the significance level of alpha is set to be 0.05. Besides, as shown in Table 4, the correlation between θ% and driving anger state is significantly negative, while the correlation between the other objective features and driving anger state are significantly positive. Hence, the IAMB algorithm is considered to be appropriate for removing irrelevant features by reducing dimension of feature set and size of input samples collected by multiple sensors.

4.2. Detection Model of Driving Anger States with Different Intensity. In this section, the effective of incremental association Markov blanket (IAMB) algorithm for feature selection and the performance of the least square support vector machine (LSSVM) model for driving anger state detection are evaluated, respectively. A training set selected from nearly half the labeled instances, consisting of 356 none anger (neutral) instances, 215 low anger instances, 107 medium

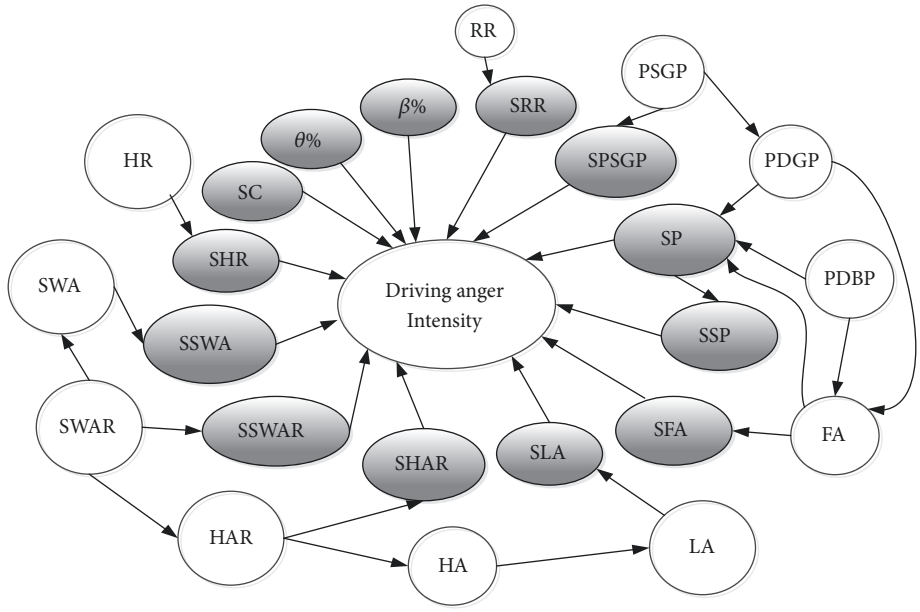

Figure 6: The Markov blanket of driving risk status.

Table 4: The correlation test for features based on IAMB algorithm.

Test method	Driving anger intensity			
	kendall's tau-b		Spearman's rho	
value	Sig. (2-tailded)	correlation coefficient	Sig. (2-tailed)	correlation coefficient
SC	0.035	0.793∗	0.029	0.835∗
SHR	0.008	0.913∗∗	0.005	0.926∗∗
SRR	0.042	0.784∗	0.036	0.805∗
θ%	0.037	-0.695*	0.032	-0.714*
β%	0.003	0.851∗∗	0.006	0.837∗∗
SPSGP	0.009	0.716**	0.012	0.753∗
SSWA	0.027	0.782∗	0.034	0.794∗
SSWAR	0.006	0.814∗∗	0.008	0.863∗∗
SHAR	0.018	0.735∗	0.017	0.796∗
SP	0.046	0.618∗	0.041	0.708∗
SSP	0.031	0.758∗	0.037	0.815∗
SFA	0.024	0.828∗	0.028	0.876∗
SLA	0.039	0.732∗	0.032	0.794∗

anger instances and 81 high anger instances are used, while the rest of the labeled instances were used as the test set. All of the algorithms are realized in Weka platform and, the data preprocess and analysis are conducted by a 64-bitWindows computer with 2.4 GHz CPU, 8 GB RAM.

4.2.1. Results of Feature Selection Based on IAMB. Several commonly used feature selection algorithms such as principle component analysis (PCA), sequential forward selection (SFS), and genetic algorithm (GA) were utilized as comparable algorithms when evaluating effectiveness of IAMB. In order to assess the effectiveness of IAMB algorithm, LSSVM model with radial basis function (RBF) kernel function whose parameters were determined by particle swarm optimization (PSO), was utilized to classify driving anger states with different intensity. As shown in Figure 7, the results indicate that accuracy (Acc) of classification of LSSVM with IAMB (i.e. 82.20%) outperforms the LSSVM models with PCA, SFS and GA. Except for that, the results illustrated in Figure 7 also clearly present that the LSSVM with IAMB is superior to the other three feature selection algorithms with respect to positive predictive accuracy (PPA), especially true positive rate (TPR) and F1.

4.2.2. Results of Detection Model Based on LSSVM. To verify the effectiveness of different classifiers with IAMB, a comparison between LSSVM and C4.5 (an advanced decision tree algorithm), Naïve Bayes classifier (NBC), SVM, k-nearest neighbor (KNN) and back propagation neural networks (BPNN) with regard to AUCs of the corresponding ROC

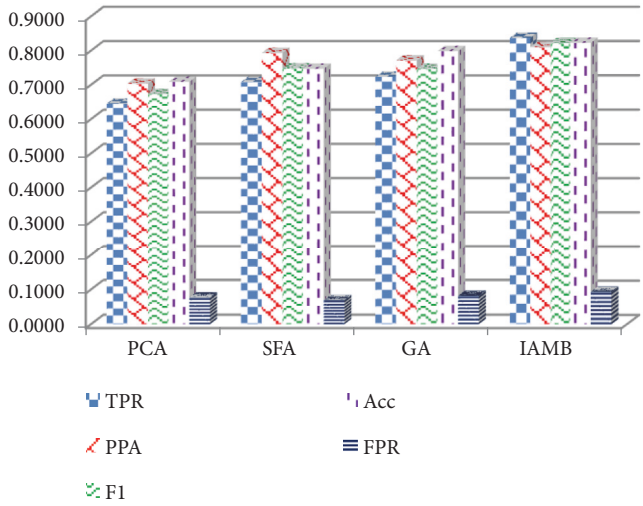

Figure 7: The effectiveness comparison between IAMB and the other three algorithms.

curves for the four driving anger states with different intensity, is shown in Figure 8.

As illustrated in Figure 8, the classification performance of IAMB model using LSSVM classifier proposed in this study from the perspective of AUC outperforms the IAMB algorithms using C4.5, NBC, KNN, SVM, and BPNN. Especially for detecting high anger state, the performance of the proposed model is significantly better ($p=0.037<0.05$) than the other five models, due to the significantly higher AUC. The average AUC of the proposed model for four driving anger states reaches 0.8764, which is the highest among the six models. Additionally, AUC of all six classifiers for driving neutral state with no anger is small than that of driving anger states with low, medium and high intensity. The reason for that may be that physiology and behavior features in driving neutral states (none anger) are significantly smaller than that of actual driving anger states.

Furthermore, for the sake of evaluating classification performance of the proposed model, the 10-fold cross validation method was implemented, with the results shown in Figure 9. As indicated in Figure 9, the proposed model of IAMB algorithm with LSSVM, achieves better performances regarding TPR, PPA, and F1, compared with IAMB algorithms with C4.5, NBC, KNN, SVM and BPNN for four driving anger states with different intensity. Particularly, the performances of the proposed model are significantly ($p=0.041<0.05$) superior to the other five models in terms of those evaluation criteria for high anger detection (see Figures 9(a)–9(d)).

Moreover, the average values of TPR, PPA, F1, FPR, AUC and total accuracy (Acc) of the proposed model together with the other five models used as a comparison were statistically analyzed for all the four driving anger states. As illustrated in Table 5, IAMB-LSSVM model achieves the best value in terms of TPR (0.8369), PPA (0.8101), F1 (0.8215), AUC (0.8764) and Acc (0.8220). Although FPR value of the proposed model is not smallest (i.e. best) among all the models, it is only 0.0749, which demonstrates that it is effective enough for detecting different driving anger states. In summary, according to the evaluation results, the LSSVM model with feature selection algorithm of IAMB has more privilege than the other five models.

5. Discussions and Conclusions

The main goal of this paper is not only to attempt a novel driving anger induction method, but also to select the most effective features which strongly correlate to driving anger states and, to explore a productive method for detecting driving anger states with different intensity. Note that, it is very necessary to detect different driving anger states, which is supportive for determining soft or hard interference through human-machine interaction by a multimodal affective car interface in advanced driving assistant system. Here, soft interference means releasing relaxed music or warning if low anger state is detected while hard interference means brake/acceleration pedal or steering wheel controlled by machine instead of human if high anger state is detected.

First, a special busy route including many heavy traffic sections was selected for the field experiments. On the experimental route, the subjects would frequently encounter some anger elicitation events such as weaving/cut-in, jaywalking/cyclist crossing, traffic congestion and waiting red lights, especially in morning or evening rush hours. The emotion elicitation effect check shows that the occurrence rate of anger induced by the elicitation events is 72.22%, much higher than that (8.08%) without elicitation. The results manifest that the novel induction method for driving anger, proposed in this study is viable through the anger elicitation events occurring in the real traffic environments and extra paid if accomplishing the test ahead of schedule. Moreover, its authenticity is superior to others under lab simulation. Coincidentally, road rage perpetration was found to be increased significantly with number of weekly kilometers driven and to be more common for drivers who always drove across heavy traffic sections than those who never drove across heavy traffic sections in Ontario, Canada [53]. Moreover, Deffenbacher et al [54]found that road rage often

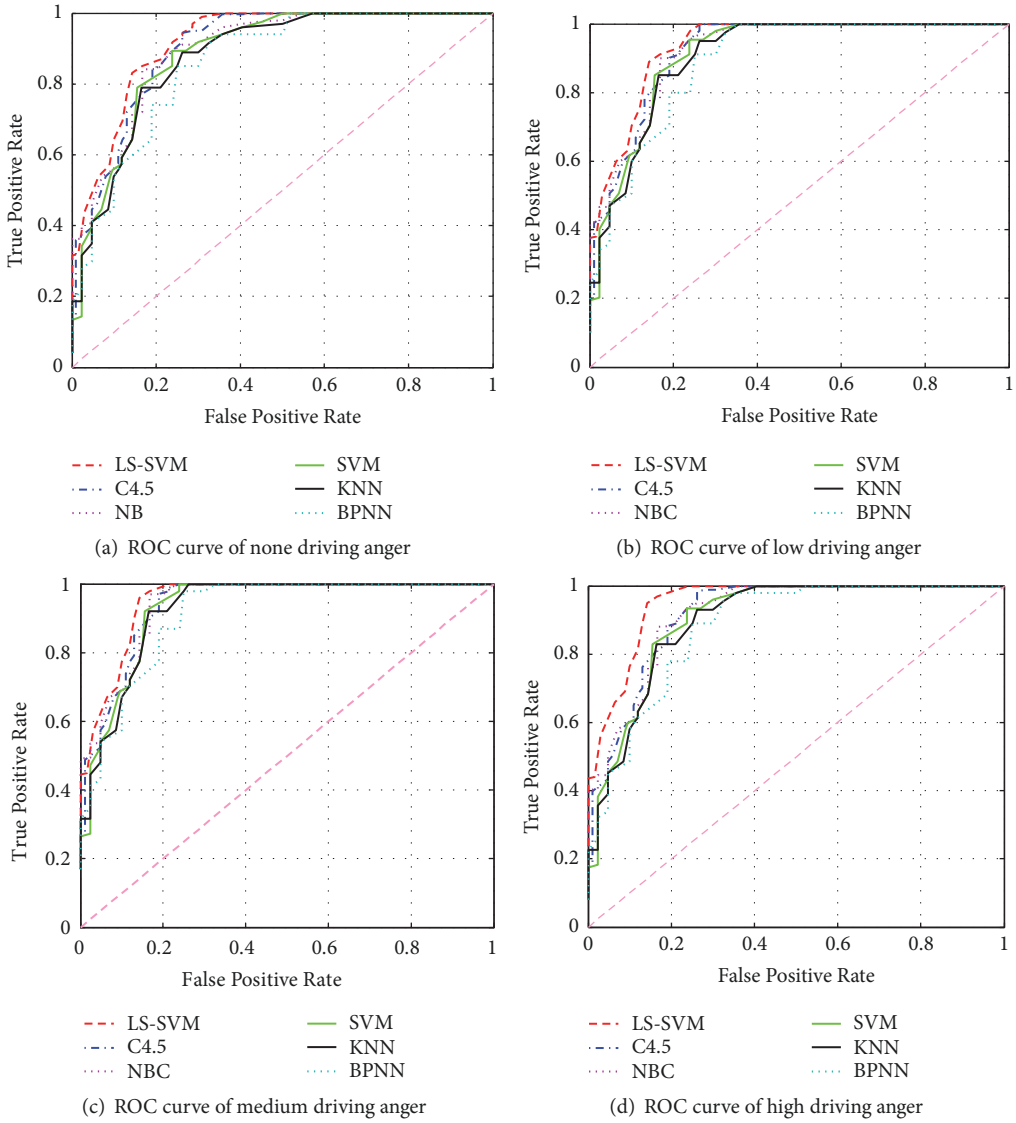

Figure 8: The AUCs of ROC curves of six classifiers for four driving anger states.

Table 5: The average classification performances of the six models for four driving anger states.

	TPR	FPR	PPA	F1	Acc	AUC
LSSVM	0.8369	0.0749	0.8101	0.8215	0.8220	0.8764
C4.5	0.7937	0.0490	0.7760	0.7828	0.8017	0.8623
NBC	0.7768	0.0627	0.7591	0.7653	0.7905	0.8439
KNN	0.7546	0.0698	0.7480	0.7487	0.7436	0.8275
SVM	0.7612	0.0582	0.7552	0.7562	0.7786	0.8376
BPNN	0.7408	0.0937	0.7458	0.7414	0.7384	0.8148

occurred under six most common scenarios in U.S. which included hostile gestures, traffic obstructions, discourtesy, illegal driving, slow driving and police presence. However, the survey results in this study show that the elicitation scenarios/events of road rage are a little different in China, especially in Wuhan, because of the differences in culture background, safety awareness, life style and traffic regulation, Therefore, the results will be supportive for dealing with the anger elicitation scenarios through making policy or developing prevention/warning technologies for traffic management or driving training authorities.

For the research of driver mental state recognition, most of previous studies roughly focus on two confused states (e.g. fatigue or not fatigue), and ignore subdivision of a certain mental state based on its intensity. What's more, only one or two types of data sets are collected for driver mental

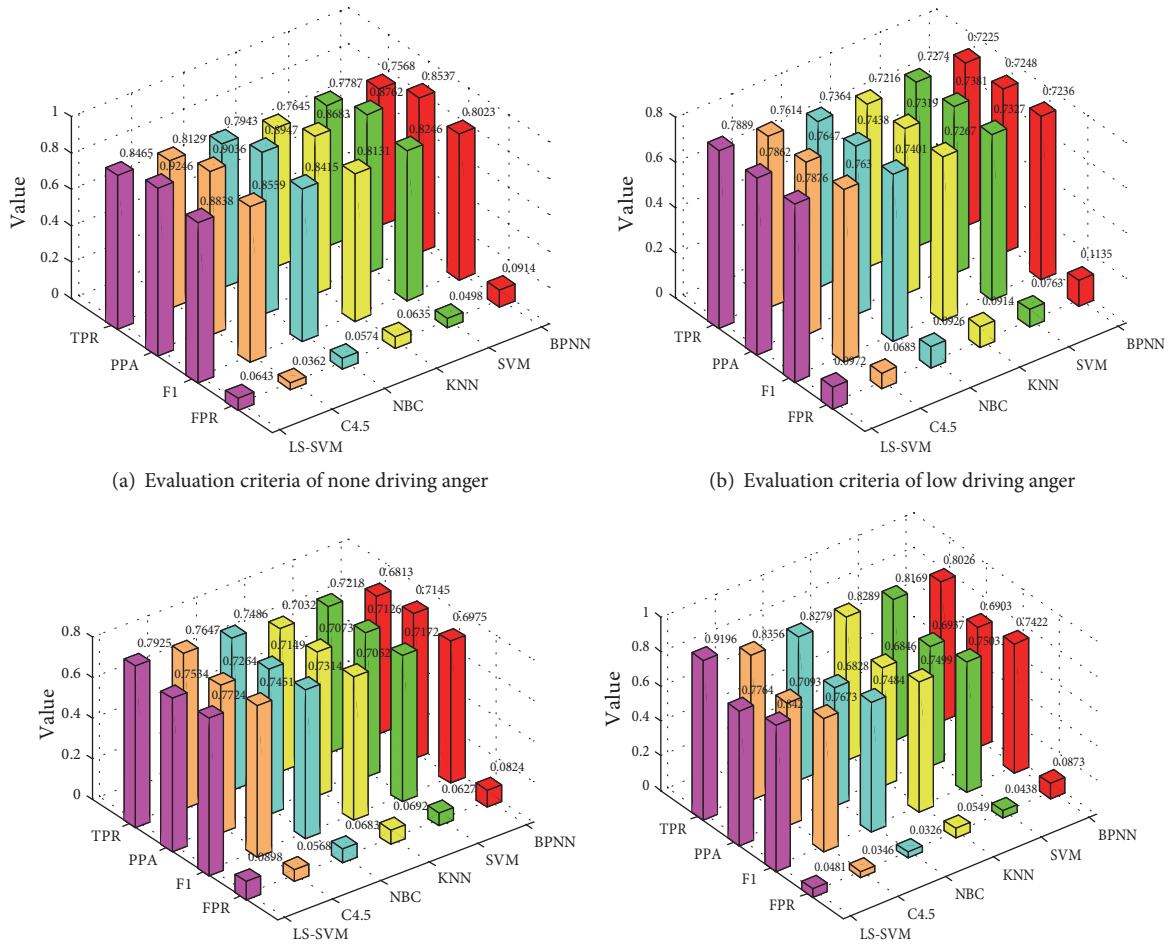

(a) Evaluation criteria of none driving anger

(b) Evaluation criteria of low driving anger

(c) Evaluation criteria of medium driving anger

(d) Evaluation criteria of high driving anger

Figure 9: The classification performance of six models for four driving anger states.

state recognition when taking financial or technical factors into consideration. However, in this study, the overall and common feature sets with regard to driver physiology, driving behaviors and vehicle motions are extracted based on the data sets acquired by the corresponding sensors.

In order to select the most effective features which significantly correlate to driving anger states, incremental association Markov blanket (IAMB) algorithm was employed in this study. According to IAMB algorithm, among the original 50 features, 13 features were selected, which consists of skin conductance (SC), SD of heart rate (SHR), SD of respiration rate (SRR), relative energy spectrum of θ band of EEG (θ%), relative energy spectrum of β band of EEG (β%), SD of pedaling speed of gas pedal (SPSGP), SD of steering wheel angle (SSWA), SD of steering wheel angle rate (SSWAR), SD of heading angle rate (SHAR), vehicle speed (SP), SD of speed (SSP), SD of forward acceleration (SFA) and SD of lateral acceleration (SLA). The Kendall's tau-b and Spearman's rho coefficient test were implemented to verify that the 13 selected features have significant impact on different driving anger states. Among the 13 features, SC, SHR, SRR, θ% and β% are physiological features which can reflect driving anger state; and SPSGP, SP, SSP, SFA are significant features to express driver's behaviors with regard to longitudinal control of vehicle under anger state, while the SSWA, SSWAR, SHAR, SLA are key features to illustrate driver's behaviors with respect to lateral control of vehicle. Therefore, the 13 features are feasible and adequate to be used for detecting driving anger states.

The study results verify that IAMB algorithm has advantage in feature selection of driving anger state over the other common algorithms: principle component analysis (PCA), sequential forward selection (SFS), and genetic algorithm (GA), in terms of TPR, PPA, F1 and Acc. Literature [24] also verifies that in comparison with principal component analysis, information gain, and class independent feature selection method, the Markov blanket-based approach can obtain better classification performance. Besides, under the same precondition using IAMB, least square support vector machine (LSSVM), introduced in this study is superior to C4.5, NBC, KNN, SVM and BPNN, regarding AUC which is a key criteria to evaluate recognition ability of a classifier. Moreover, IAMB algorithm with LSSVM, achieves better performances with respect to TPR, PPA, and F1, compared with IAMB algorithms with the other five widely used models when classifying the four driving anger states with

different intensity. Specially, the proposed model significantly outperforms the five models when detecting high driving anger state, which may be due to considerable changes of the selected features in this state. Additionally, the total accuracy of IAMB-LSSVM for detecting all driving anger states reaches 82.20%, which is 2.03%, 3.15%, 4.34%, 7.84% and 8.36% higher than IAMB using C4.5, NBC, SVM, KNN and BPNN, respectively. Although FPR value of the proposed model is not best among all the models, it is only 0.0749, implying that it is effective enough for detecting driving anger states

Nevertheless, due to the limitations in this study, some deep research can be conducted in future. Firstly, as only male drivers were enrolled for the sake of statistical power, we should add female drivers in future to enhance the generalizability of the detection model presented in this study. Nonetheless, female drivers were found to be angrier than males when facing traffic obstruction, and they were inclined to conduct more adaptive expression and less aggression behaviors, when they became angry while driving [55]. Then, a more congested route with more traffic jams, more red light waiting, more pedestrians' crossing street (jaywalking) and more slowly moving cars with high traffic density, or more large buses which keep the participants from overtaking or seeing around, can be designed to trigger more anger for female drivers. And except for behavior measurements, some other measurements like physiology, face or speech expression indicators should be focused to study driving anger expression differences. Secondly, the field experiments were only performed in Wuhan which is a representative central metropolis in China. Then, considering the differences of anger elicitation scenarios and expression ways due to life style, driving style, safety awareness and traffic regulation obedience, the subsequent experiments should be performed in other representative and regional cities like Beijing, Guangzhou, Chengdu, and so on. Thirdly, the sensors gathering physiological signals were straightforwardly attached to driver's skin surface, which probably interfere with the driver's natural driving behavior. Hence, some non-intrusive wearable apparatus should be implemented for collecting physiological signals in future. In addition, the drivers' personality/demographic characteristics such as age, gender, temperament, driving experience and driving style have close relationships with driving anger states [56–58]. Nonetheless, the relationships have not been considered due to the relatively small number of participants.

Data Availability

The data used to support the findings of this study are available from the corresponding author upon request.

Conflicts of Interest

The authors declare no conflict of interest.

Acknowledgments

The present study is supported by the project funded by Young Doctor Fund of Social Science program of Jiang Xi Province (17BJ42).

References

[1] W. Wang, F. Sun, Q. Cao, and S. Liu, *Driving Behavior Theory and Its Application in Road Traffic System*, Science Press, Beijing, China, 2001.

[2] K. Brookhuis, D. De Waard, and B. Mulder, "Measuring driving performance by car-following in traffic," *Ergonomics*, vol. 37, no. 3, pp. 427–434, 1994.

[3] E. R. Dahlen, R. C. Martin, K. Ragan, and M. M. Kuhlman, "Driving anger, sensation seeking, impulsiveness, and boredom proneness in the prediction of unsafe driving," *Accident Analysis & Prevention*, vol. 37, no. 2, pp. 341–348, 2005.

[4] C. Wu and L. Hu, "Review on the study of Motorists' driving anger," *China Safety Science Journal*, vol. 20, no. 7, pp. 3–8, 2010.

[5] NHTSA, *Traffic safety facts: a compilation of motor vehicle crash data from the fatality analysis reporting system and the general estimates system*, U.S.A Department of Transportation, 2011.

[6] H. Lei, *The Characteristics of Angry Driving Behaviors and Its Effects on Traffic Safety [Master's, thesis]*, Wuhan University of Technology, 2011.

[7] S. Sheila, M. Alanna, E. Mohammad, K. Mohammad, and W. Karen, "Aggressive driving and road rage behaviors on freeways in san diego," *Transp Res Record*, vol. 1724, pp. 7–13, 2000.

[8] NHTSA, *Traffic Safety Facts 2007: A Compilation of Motor Vehicle Crash Data from the Fatality Analysis Reporting System and the General Estimates System*, National Highway Traffic Safety Administration, Washington DC, Wash, USA, 2007.

[9] T. Lajunen and D. Parker, "Are aggressive people aggressive drivers? A study of the relationship between self-reported general aggressiveness, driver anger and aggressive driving," *Accident Analysis & Prevention*, vol. 33, no. 2, pp. 243–255, 2001.

[10] E. C. Suarez and R. B. Williams, "Situational determinants of cardiovascular and emotional reactivity in high and low hostile men," *Psychosomatic Medicine*, vol. 51, no. 4, pp. 404–418, 1989.

[11] L. Kessous, G. Castellano, and G. Caridakis, "Multimodal emotion recognition in speech-based interaction using facial expression, body gesture and acoustic analysis," *Journal on Multimodal User Interfaces*, vol. 3, no. 1, pp. 33–48, 2010.

[12] P. N. Juslin and J. A. Sloboda, *Handbook of Music and Emotion: Theory, Research, Applications*, Oxford University Press, New York, NY, USA, 2010.

[13] H. Lei, X. Yan, and C. Wu, "The characteristic of vehicle speed under angry driving in china," in *Proceedings of the Second International Conference on Transportation Information and Safety*, pp. 1542–1547, Wuhan, China.

[14] R. Abdu, D. Shinar, and N. Meiran, "Situational (state) anger and driving," *Transportation Research Part F: Traffic Psychology and Behaviour*, vol. 15, no. 5, pp. 575–580, 2012.

[15] H. Cai and Y. Lin, "Modeling of operators' emotion and task performance in a virtual driving environment," *International Journal of Human-Computer Studies*, vol. 69, no. 9, pp. 571–586, 2011.

[16] K. Oeltze and C. Schie, "Benefits and challenges of multi-driver simulator studies," *IET Intelligent Transport Systems*, vol. 9, no. 6, pp. 618–625, 2015.

[17] D. Zhang, B. Wan, and D. Ming, "Research progress on emotion recognition based on physiological signals," *Journal of Biomedical Engineering*, vol. 32, no. 1, pp. 229–234, 2015.

[18] E. Sönmez and A. Songül, "A facial component-based system for emotion classification," *Turkısh Journal Of Electrıcal Engıneerıng Computer*, vol. 24, pp. 1663–1673, 2016.

[19] A. Shahzadi, A. Ahmadyfard, A. Harimi, and K. Yaghmaie, "Speech emotion recognition using nonlinear dynamics features," *Turkish Journal of Electrical Engineering & Computer Sciences*, vol. 23, pp. 2056–2073, 2015.

[20] J. Healey, *Wearable and Automotive Systems for Affect Recognition from Physiology [Ph.D. thesis]*, MIT, Cambridge, Mass, USA, 2000.

[21] J. Wagner, J. Kim, and E. Andre, "From Physiological signals to emotion: implementing and comparing selected methods for feature extraction and classification," in *Proceedings of the 2005 IEEE International Conference on Multimedia and Expo.*, pp. 940–943, Amsterdam, Netherlands.

[22] B.-G. Lee, B.-L. Lee, and W.-Y. Chung, "Mobile healthcare for automatic driving sleep-onset detection using wavelet-based EEG and respiration signals," *Sensors*, vol. 14, no. 10, pp. 17915–17936, 2014.

[23] N. Wu, H. Jiang, and G. Yang, "Emotion recognition based on physiological signals," *Advances in Brain Inspired Cognitive Systems*, vol. 7366, pp. 311–320, 2012.

[24] J. Chen, A. G. Wang, K. X. Wang, N. An, and L. Li, "Speech emotion recognition with class-dependent feature selection methods," *Microelectronics & Computer*, vol. 33, pp. 92–96, 2016.

[25] L.-X. Yan, Z. Huang, D.-Y. Zhu, Z.-J. Chen, and B. Ran, "Driving risk status identification based on markov blanket hidden naive bayes," *Journal of Jilin University (Engineering and Technology Edition)*, vol. 46, no. 6, pp. 1851–1857, 2016.

[26] B. Han, X.-W. Chen, and Z. Talebizadeh, "FEPI-MB: identifying SNPs-disease association using a Markov Blanket-based approach," *BMC Bioinformatics*, vol. 12, p. S3, 2011.

[27] A. J. Flidlund and E. Z. Izard, *Electromyographic Studies of Facial Expressions of Emotions and Patterns of Emotions*, Guilford Press, New York, NY, USA, 1983.

[28] J. Wang and Y. Gong, "Normalizing multi-subject variation for drivers' emotion recognition," in *Proceedings of the IEEE International Conference on Multimedia and Expo (ICME)*, pp. 354–357, New York, NY, USA, June 28-July 3 2009.

[29] C. D. Katsis, Y. Goletsis, G. Rigas, and D. I. Fotiadis, "A wearable system for the affective monitoring of car racing drivers during simulated conditions," *Transportation Research Part C: Emerging Technologies*, vol. 19, no. 3, pp. 541–551, 2011.

[30] X. Fan, L. Bi, and Z. Chen, "Using EEG to detect drivers' emotion with Bayesian networks," in *Proceedings of the International Conference on Machine Learning and Cybernetics (ICMLC)*, pp. 1177–1181, Qingdao, China, July 2010.

[31] L. Malta, C. Miyajima, N. Kitaoka, and K. Takeda, "Analysis of real-world driver's frustration," *IEEE Transactions on Intelligent Transportation Systems*, vol. 12, no. 1, pp. 109–118, 2011.

[32] A. Lanatà, G. Valenza, A. Greco et al., "How the Autonomic nervous system and driving style change with incremental stressing conditions during simulated driving," *IEEE Transactions on Intelligent Transportation Systems*, vol. 16, no. 3, pp. 1505–1517, 2015.

[33] G. Rigas, Y. Goletsis, and D. I. Fotiadis, "Real-time driver's stress event detection," *IEEE Transactions on Intelligent Transportation Systems*, vol. 13, no. 1, pp. 221–234, 2012.

[34] A. Reyes-Muñoz, M. C. Domingo, M. A. López-Trinidad, and J. L. Delgado, "Integration of body sensor networks and vehicular ad-hoc networks for traffic safety," *Sensors*, vol. 16, no. 107, pp. 1–29, 2016.

[35] D. Shinar and R. Compton, "Aggressive driving: an observational study of driver, vehicle, and situational variables," *Accident Analysis & Prevention*, vol. 36, no. 3, pp. 429–437, 2004.

[36] P. Wan, C. Wu, Y. Lin, and X. Ma, "Optimal threshold determination for discriminating driving anger intensity based on EEG wavelet features and ROC curve analysis," *Information (Switzerland)*, vol. 7, no. 3, Article ID 7030052, 2016.

[37] P. Wan, C. Wu, Y. Lin, and X. Ma, "On-road experimental study on driving anger identification model based on physiological features by ROC curve analysis," *IET Intelligent Transport Systems*, vol. 11, no. 5, pp. 290–298, 2017.

[38] B. Xu, A. Song, and G. Zhao, "Design and evaluation of a motor imagery electroencephalogram controlled robot system," *Advances in Mechanical Engineering*, pp. 1–11, 2015.

[39] D. Koller and M. Sahami, "Toward optimal feature selection," in *Proceedings of 13th International Conference on Machine Learning*, pp. 211–232, Bari, Italy, 1996.

[40] Y. Zhang and Z. Zhang, "Feature subset selection with cumulate conditional mutual information minimization," *Expert Systems with Applications*, vol. 39, no. 5, pp. 6078–6088, 2012.

[41] S. Fu and M. C. Desmarais, "Markov blanket based feature selection: A review of past decade," in *Proceedings of the World Congress on Engineering, WCE 2010*, pp. 321–328, 2010.

[42] C. F. Aliferis, A. Statnikov, and I. Tsamardinos, "Local causal and markov blanket induction for causal discovery and feature selection for classification part II: analysis and extensions," *Journal of Machine Learning Research*, vol. 11, pp. 235–284, 2010.

[43] I. Tsamardinos, C. F. Aliferis, and A. Statnikov, "Algorithms for large scale Markov blanket discovery," *American Association for Artificial Intelligence*, pp. 376–381, 2003.

[44] J. Lee and C.-H. Jun, "Classification of high dimensionality data through feature selection using Markov blanket," *Industrial Engineering & Management Systems*, vol. 14, no. 2, pp. 210–219, 2015.

[45] C. Cortes and V. Vapnik, "Support-vector networks," *Machine Learning*, vol. 20, no. 3, pp. 273–297, 1995.

[46] J. A. K. Suykens and J. Vandewalle, "Least squares support vector machine classifiers," *Neural Processing Letters*, vol. 9, no. 3, pp. 293–300, 1999.

[47] J. A. K. Suykens, J. De Brabanter, L. Lukas et al., "Weighted least squares support vector machines: robustness and sparce approximation," *Neurocomputing*, vol. 48, pp. 85–105, 2002.

[48] J. Kennedy and R. Eberhart, "Particle swarm optimization," in *Proceedings of the IEEE International Conference on Neural Networks*, pp. 1942–1948, 1995.

[49] Y. Shi and R. C. Eberhart, "Parameter selection in particle swarm optimization," *Lecture Notes in Computer Science*, vol. 1447, pp. 591–600, 1998.

[50] C. Sun, J. He, and H. Xiao, "A new performance evaluation method based on ROC curve," *Radar Science and Technology*, vol. 5, no. 1, pp. 17–21, 2007.

[51] X. H. Zhao, H. J. Du, and J. Rong, "Research on identification method of fatigue driving based on ROC curves," *Journal of Transport Information*, vol. 32, no. 5, pp. 88–94, 2014.

[52] T. Bechtel, L. Capineri, C. Windsor, and M. Inagaki, "Comparison of ROC curves for landmine detection by holographic radar with ROC data from other methods," in *Proceedings of the 8th International Workshop on Advanced Ground Penetrating Radar, IWAGPR 2015*, 4, 1 pages, Florence, Italy, July 2015.

[53] R. G. Smart, G. Stoduto, R. E. Mann, and E. M. Adlaf, "Road rage experience and behavior: Vehicle, exposure, and driver factors," *Traffic Injury Prevention*, vol. 5, no. 4, pp. 343–348, 2004.

[54] J. L. Deffenbacher, "Anger, aggression, and risky behavior on the road: A preliminary study of urban and rural differences,"

Journal of Applied Social Psychology, vol. 38, no. 1, pp. 22–36, 2008.

[55] B. González-Iglesias, J. A. Gómez-Fraguela, and M. Á. Luengo-Martín, "Driving anger and traffic violations: Gender differences," *Transportation Research Part F: Traffic Psychology and Behaviour*, vol. 15, no. 4, pp. 404–412, 2012.

[56] D. Herrero-Fernández, "Psychometric adaptation of the driving anger expression inventory in a spanish sample: Differences by age and gender," *Transportation Research Part F: Traffic Psychology and Behaviour*, vol. 14, no. 4, pp. 324–329, 2011.

[57] Z. Feng, Y. Lei, H. Liu et al., "Driving anger in China: A case study on professional drivers," *Transportation Research Part F: Traffic Psychology and Behaviour*, vol. 42, pp. 255–266, 2016.

[58] Y. Ge, W. Qu, C. Jiang, F. Du, X. Sun, and K. Zhang, "The effect of stress and personality on dangerous driving behavior among Chinese drivers," *Accident Analysis & Prevention*, vol. 73, pp. 34–40, 2014.